JOURNAL OF PROPULSION AND POWER
Vol. 13, No. 4, July–August 1997

Mean Stator Loading Effect on the Acoustic Response of a Rotating Cascade

Scott Sawyer* and Sanford Fleeter†
Purdue University, West Lafayette, Indiana 47907

Discrete-frequency tones generated by unsteady blade row interactions are of particular concern in the design of advanced turbine engines. With a rotor–stator mounted in a duct, only certain specific spatial modes are generated by the rotor–stator interaction, where the generated modes are a function of the number of rotor blades and stator vanes. In addition, only some of these modes propagate to the far field, with the rest decaying before reaching the far field. Thus, it is only those spatial modes that propagate to the far field that represent the discrete-frequency noise received by an observer. This paper's aim is to determine the influence of steady stator loading on the acoustic response of an annular cascade. To accomplish this, the existence of the propagating modes generated by a rotor–stator interaction must first be verified. Microphones placed in an axial plane in the outer annulus of the inlet of the Purdue Annular Cascade Research Facility are sampled simultaneously over one rotor revolution, and an ensemble-averaged data set is acquired. With the microphone signals treated as a function of time and space, dual Fourier transforms are utilized to determine the magnitude of the spatial modes at multiples of blade pass frequency. The wave equation is used to predict the propagation characteristics of these modes in the inlet duct. The two predicted propagating modes were found to have significantly higher amplitudes than modes that were predicted to decay, or were not to be generated by the rotor–stator interaction, and steady stator loading had a profound influence on acoustic response of the cascade. The acoustic response at blade pass and twice blade pass frequency increased by more than 20 dB for angles of attack ranging from −20 to 25 deg.

Nomenclature

a_∞ = freestream speed of sound
k_θ = tangential wave number
$k_{\theta,\text{critical}}$ = critical Nyquist mode
k_μ = eigenvalue
k_ξ = axial wave number
M = axial mean flow Mach number
N = number of microphones
N_{Blades} = number of rotor blades
N_{Vanes} = number of stator vanes
n = rotor harmonic
P = spatial transform of acoustic pressure
p = acoustic pressure
r = radial coordinate
U_∞ = mean axial velocity
v = stator index, 0, 1, . . . , $N_{\text{Vanes}} - 1$
x = axial direction
α = mean stator angle of attack
θ = circumferential coordinate
ξ = axial coordinate
Ω = rotor circular frequency
Ω_p = pressure pattern phase speed
ω = multiple of blade pass frequency $nN_{\text{Blades}}\Omega$

Introduction

IN the design of advanced gas-turbine engines, aeroacoustics is an increasingly important issue. Long-term performance requirements of advanced design engines include increased fuel efficiency, decreased weight, and improved reliability and maintainability, while being competitively priced. Engine certification requires meeting prevailing noise regulations, such as the U.S. FAR 36 Stage 3 rules, which are to be implemented through the end of this decade. In addition, more stringent noise level guarantees are often required of the engine manufacturer by airlines to meet tougher local airport noise requirements. There is a near certainty that more stringent Stage 4 requirements will require an additional reduction of up to 5 effective perceived noise level (EPNLdB).

As engines with higher bypass ratios have been introduced, turbomachinery noise, i.e., fan, compressor, and turbine-generated noise, has become more important, with jet exhaust mixing noise contributing less and less to the total engine noise signature. For example, for current high-bypass-ratio engines (bypass ratios of 5:1 to 6:1), fan noise dominates the total noise on approach and takeoff. New ultra-high-bypass ratio ducted-fan engines (bypass ratios greater than 10:1) that will have an even greater fan noise component at lower frequencies, with a significant reduction in the contribution of jet noise to the total engine noise signature, will be introduced over the next few years.

Figure 1 shows the primary noise sources for a high-bypass turbofan engine: the fan, the low-pressure or booster compressor, and the low-pressure turbine.[1,2] Their noise signatures include a broadband noise level with large spikes or tones at multiples of the blade passing frequency. For subsonic fans, the acoustic spectrum discrete tones usually have narrow bandwidth amplitudes 10–15 dB above the broadband level. The discrete-frequency tones are generated by periodic blade row unsteady aerodynamic interactions between adjacent blade rows. Namely, turbomachine blade rows are subject to spatially nonuniform inlet flowfields resulting from either potential or viscous wake interactions. Potential flow interactions result from variations in the pressure field associated with the blades of a given row and their effect on the blades of a neighboring row moving at a different rotational speed. This type of interaction is of concern when the axial spacing between neighboring blade rows are small or flow Mach numbers are high.

Received May 1, 1995; revision received Feb. 5, 1997; accepted for publication April 15, 1997.

*AFRAPT Trainee, School of Mechanical Engineering, 1003 Chaffee Hall. Student Member AIAA.

†McAllister Distinguished Professor, School of Mechanical Engineering, 1003 Chaffee Hall. Associate Fellow AIAA.

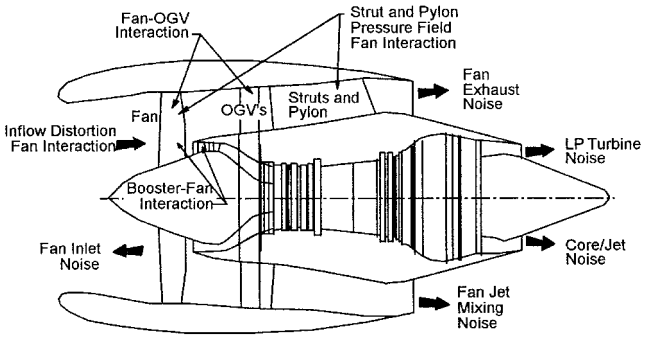

Fig. 1 Sources of turbomachine noise.

Wake interactions result from the impingement of wakes shed by one or more upstream rows upon the flow through a downstream blade row. This type of interaction can persist over considerable axial distances. Both of these interactions result in the generation of acoustic waves that may propagate unattenuated and also interact with other blade rows.

Current noise control and reduction methods for high-bypass turbofan engines usually are a combination of turbomachinery noise source control and suppression. Source control is accomplished by increasing axial spacing between adjacent blade rows and by selecting blade and vane number combinations to produce cutoff, whereby the highest-energy acoustic modes decay exponentially with distance along the duct. Source suppression is achieved with acoustic liners in the fan inlet and exhaust ducts and the core exhaust duct.

The increasing bypass ratios of advanced turbofan engines leads to increased fan diameters. However, nacelle length is to be kept at the current bypass ratio size, not scaled with diameter. Thus, inlet and exhaust duct length-to-diameter ratios will be smaller and current liner design techniques will provide less noise suppression. As the fan diameter increases, the blading becomes larger, and a severe weight penalty is realized if axial spacing is maintained for source control. Further, the trend toward low-blade-number, wide-chord fan designs is a further deterrence to maintaining large spacing/chord ratios. Larger diameters, lower blade numbers, and lower tip speeds all produce lower blade-passing frequencies that require deeper treatment liners to achieve comparable suppression. Low drag configurations require large-diameter nacelles to be thin. As a result, current liner treatment designs will provide significantly less source suppression.

In summary, higher-bypass-ratio engines will require more source noise control by designing to avoid high amplitude noise vs just suppressing noise using liner technologies. Progress in gas-turbine noise reduction design is dependent on a better understanding of turbomachinery noise, specifically far-field discrete-frequency noise.

For a turbomachine stage, only specific spatial acoustic modes are generated by the rotor–stator interactions. To identify noise source mechanisms and for duct treatment design and noise control, it is important to measure this modal sound structure. Levy and Canard-Caruana[3] performed a modal analysis of the sound field in the inlet duct of a model turbofan to discriminate the rotor–stator interaction modes. They found that a lining optimized for blade passage frequency could produce considerably more reduction than a conventional lining. Joppa[4] made turbofan engine inlet duct propagation measurements using equally spaced microphones mounted flush with the duct wall. Circumferential and axial microphone arrays were analyzed by an analog heterodyne procedure and a Fourier transform in the spatial domain, with the modal data used to design an acoustic liner with improved efficiency as compared to the equal energy per mode assumption. Weir and Marsan,[5] utilizing a one-half size fan, verified the low noise design of a new fan by identifying the modal orders and amplitudes of each propagating mode, extrapolating these to the far field, and correlated these results with far-field noise measurements.

Heidelberg and Hall[6] and Hall et al.[7] made comprehensive measurements of the spinning acoustic mode structure in the inlet of the advanced ducted propeller using a unique method in which a continuously rotating microphone system was used. Spatial acoustic mode levels were measured at a series of radial locations using the Doppler frequency shift produced by a rotating inlet microphone probe. Radial content was then calculated using a least-squares curve fit with the measured distribution for each spatial mode.

For a turbomachine stage, a rotor and stator mounted in a duct, only specific spatial acoustic modes are generated by the rotor–stator interaction, with these modes determined by the number of rotor blades and stator vanes. In addition, only some of these modes propagate to the far field, with the rest decaying with axial distance. Thus, it is those spatial modes that propagate to the far field that represent the majority of discrete-frequency noise received by an observer.

This paper is directed at investigating the effect of mean stator loading on acoustic response of an annular cascade. This is accomplished in the Purdue Annular Cascade Research Facility equipped with a rotor–stator mounted in the test section and a circumferential array of 10 microphones mounted in the outer wall of the inlet. The microphone array is sampled simultaneously over one rotor revolution, and an optical encoder on the rotor is used to obtain an ensemble-averaged data set. The microphone signals are treated as a function of time and space, and a dual Fourier transform is applied to determine the magnitude of the spatial modes as a function of frequency. The wave equation is used to predict the propagation characteristics of these modes in the inlet duct. Unsteady pressure measurements are made to verify the existence of the propagating acoustic modes generated by the rotor–stator interaction and to then investigate the effect of mean stator loading on the acoustic response.

Discrete-Frequency Noise Generation

The model to analyze the discrete-frequency noise generated in a turbomachine considers a rotor and stator in a duct.[8]

The flow in an annular duct is described by the three-dimensional wave equation, derived by considering the flow to be inviscid and compressible with small unsteady perturbations:

$$\left(\frac{\partial}{\partial t} + U_\infty \frac{\partial}{\partial \xi}\right)^2 p = a_\infty^2 \left(\frac{\partial^2}{\partial r^2} + \frac{1}{r}\frac{\partial}{\partial r} + \frac{1}{r^2}\frac{\partial^2}{\partial \theta^2} + \frac{\partial^2}{\partial \xi^2}\right) p \quad (1)$$

The wave equation is variable separable, and the acoustic pressure is given by

$$p(\xi, r, \theta, t) = \bar{p}(k_\mu r)\exp[i(k_\xi \xi + k_\theta \theta - \omega t)] \quad (2)$$

where $\bar{p}$ is a linear combination of Bessel functions.

To determine k_θ, a rotor and stator in a duct are considered. The acoustic response of the stator is given as the superposition of spinning modes generated at multiples of the blade pass frequency. The number of lobes of the spinning pressure pattern, termed the spatial mode order, is a function of the number of rotor blades and stator vanes. Tyler and Sofrin[8] find

$$k_\theta = nN_{\text{Blades}} + mN_{\text{Vanes}} \quad (3)$$

where n is the rotor harmonic and $m = 0, \pm 1, \pm 2, \ldots$ is an arbitrary integer. The angular velocity of the pressure pattern is characterized by the phase speed $\Omega_p = nN_{\text{Blades}}\Omega/k_\theta$.

The only modes generated by the rotor–stator interaction are specified by $k_\theta = nN_{\text{Blades}} + mN_{\text{Vanes}}$. Note that while k_θ represents the spatial distribution of the pressure, only integer values of k_θ are valid. Note that a negative value for k_θ represents a backward traveling wave, i.e., the wave rotates in a direction opposite that of rotor rotation.

Far-Field Discrete-Frequency Noise

Although all of the acoustic pressure spatial modes of order $k_\theta = nN_{\text{Blades}} + mN_{\text{Vanes}}$ are generated by the rotor–stator interaction at the harmonics of blade passage frequency $\omega = nN_{\text{Blades}}\Omega$, only some of these modes propagate to the far field, with the remainder decaying before reaching the far field. Thus, it is only those spatial modes propagating to the far field that represent the discrete-frequency noise received by an observer. The propagation, decay, or resonance of the acoustic wave in the duct is determined by the axial wave number, specifically the expression under the radical of

$$k_\xi = \frac{k_\omega M}{1 - M^2} \pm \sqrt{\left(\frac{k_\omega M}{1 - M^2}\right)^2 + \frac{k_\omega^2 - k_\mu^2}{1 - M^2}} \tag{4}$$

$k_\omega^2 - k_\mu^2(1 - M^2) > 0$: There are two real k_ξ values corresponding to two propagating pressure waves, one upstream and the other downstream.

$k_\omega^2 - k_\mu^2(1 - M^2) < 0$: There are two complex k_ξ values corresponding to two decaying waves, one upstream and the other downstream.

$k_\omega^2 - k_\mu^2(1 - M^2) = 0$: This is a resonance condition, with the resonant frequency known as the cutoff frequency because below the cutoff frequency the pressure waves decay in the axial direction or are cut off.

Experimental Facility and Instrumentation

The experiments were performed in the Purdue Annular Cascade Research Facility (Fig. 2). This facility is a low-speed, open-loop, draw-through-type wind tunnel capable of test section velocities of 220 ft/s ($M \cong 0.2$). The flow, conditioned by a honeycomb section and an acoustically treated inlet plenum, accelerates though a bellmouth inlet to the constant area annular test section. The flow exiting the test section is diffused into a large acoustically treated exit plenum. The flow is drawn through the facility by a 300-hp centrifugal fan located downstream of the exit plenum, and the rotor is driven by a 10-hp ac motor with a variable speed drive that is installed in the centerbody. Thus, the rotor speed and the flow rate are independently controlled, and run conditions for all cases were held constant. The rotor shaft rotation was maintained at 800 rpm, and the axial velocity in the test section was held constant at 175 ft/s.

An array of 10 PCB Piezotronics model 103A piezoelectric microphones with uniform circumferential spacing are mounted via static pressure taps in the outer wall of the inlet annulus (Fig. 2). The microphones are calibrated as installed in the rig and are found to have a flat frequency response from 100 to over 1000 Hz. The errors in the unsteady pressure measurements are estimated to be below 5%. The microphones are in an axial plane two rotor chord lengths (30.48 cm, 12 in.) upstream of the rotor. The Nyquist critical mode is 5 for the 10-microphone array, with all signals having a spatial mode order above the Nyquist critical mode aliased below the Nyquist mode. A Scanivalve Corporation pressure measuring system is utilized for measurement of the stator vane steady surface pressures. The system features a 1-psi linear-sensitivity transducer, a pressure multiplexer, and a ±5.0-V output signal conditioner. Calibrations were performed using a water manometer.

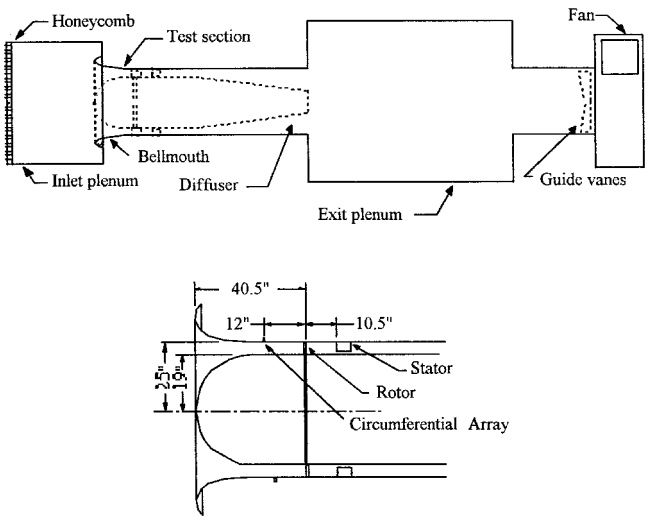

Fig. 2 Purdue Annular Cascade Facility.

The annular test section was configured with an 800-rpm rotor with 16 3-in.-wide perforated plates upstream of a stator with 18 NACA 65A612 cambered airfoils with a 15.24-cm (6.00-in.) chord, resulting in a rotor shaft pass frequency of 13.3 Hz and a blade pass frequency of 213.3 Hz. The perforated plates are installed perpendicular to the rotor axis and impart no flow turning. The perforated plate wake generators that provide a primarily vortical gust were chosen in this study for their ease of use. An optical pickup on the rotor shaft was utilized to determine the rotor pass speed, with the stator mean incidence angles varied from −20 to 25 deg relative to the axial flow at the stator inlet.

Data Acquisition

Acquisition and digitization of the microphone signals and the shaft trigger signal is accomplished using three National Instruments NB-A2000 analog-to-digital boards installed in an Apple Macintosh Quadra 950 computer. This system allows the simultaneous acquisition of 12 channels of data, initiated by the shaft trigger signal. An ensemble of 256 data points are acquired over one rotor revolution, and 200 ensembles are then averaged to reduce the random noise not linked to the rotor passage.

Signal Processing

The inlet microphone array measurements must be decomposed to determine the amplitude of the acoustic modes that make up the signal. The acoustic modes generated at blade passage frequency and twice blade passage frequency are of primary concern. To properly apply the spatial transform, the frequency of interest must be separated from the temporal signal and the transform must operate on complex data to separate the forward- and backward-spinning modes. Therefore, two Fourier transforms are required to determine the acoustic response as a function of both frequency and spatial mode. The spatial and temporal transforms are accomplished through the discrete Fourier transform.

Dual Spatial-Temporal Domain Discrete Fourier Transform

Discrete Fourier transforms are performed in time and space to calculate the amplitude of the acoustic modes at the frequencies of primary concern, blade passage and twice blade passage frequency. The dual Fourier transforms are given by

$$P(n_{\text{rev}}\Delta f, k_\theta) = \frac{2}{NN_s} \sum_{j=0}^{N_s-1} \sum_{l=0}^{N-1} p_{j,l} \exp[-i2\pi(k_\theta l/N - n_{\text{rev}} j/N_s)] \tag{5}$$

where $P(n\Delta f, k_\theta)$ amplitude of the acoustic mode at frequency $n_{\text{rev}}\Delta f$ and spatial mode k_θ, N_s is the number of samples in time, and $p_{j,l}$ is the jth sample of the lth microphone. Data are taken over one rotor revolution so that Δf is equal to the rotor shaft pass frequency, and n_{rev} is the rotor shaft order. Only positive frequencies are considered, and the discrete transform is preceded by a 2.

Nyquist Sampling Criteria

The Fourier analysis of a continuous signal sampled at discrete locations has resolution limited by the number of microphones, with a signal that consists of a spatial mode higher than the Nyquist mode aliased into a mode below the Nyquist mode.

A minimum of two samples of a sinusoidal signal is required to determine spatial mode order and signal amplitude. Applying the theory of Nyquist frequency to a spatial transform yields a critical spatial mode $k_{\theta,\text{critical}}$ which is related to the number of microphones. The Nyquist critical spatial mode is given by $N/2$.

The discrete transform can determine the amplitude and phase of the spatial modes below the Nyquist mode. A signal with spatial mode outside of the range $-k_{\theta,\text{critical}}$ to $k_{\theta,\text{critical}}$ will be aliased into that range. If a signal has a spatial mode order higher than the Nyquist critical mode order, the signal will be aliased into a mode below the critical mode order. For $k_\theta > N/2$, define k'_θ such that $k_\theta = N + k'_\theta$. The discrete transform is

$$P(n_{\text{rev}}\Delta f, k_\theta) = \frac{2}{NN_s}\sum_{j=0}^{N_s-1}\sum_{l=0}^{N-1} p_{j,l}e^{i2\pi l} \times \exp[-i2\pi(k'_\theta l/N - n_{\text{rev}}j/N_s)] = P(n_{\text{rev}}\Delta f, k'_\theta)$$

Thus, the discrete transform of a spatial mode k_θ that is higher than the critical Nyquist mode is aliased into a mode k'_θ below the critical Nyquist mode. Likewise, the discrete transform of a spatial mode k_θ that is lower than the critical Nyquist mode is aliased into mode k'_θ at the critical Nyquist mode. Figure 3 depicts the aliasing of an undersampled signal. The modes above the critical Nyquist mode are erroneously aliased into modes that are below the critical Nyquist mode.

For these experiments, with an array of 10-PCB 103A microphones, the Nyquist critical mode is 5 for the 10 microphone array. Signals that have a spatial mode order above the Nyquist critical mode will be aliased below the Nyquist mode.

Results

To verify the existence of turbomachine stage propagating acoustic modes and investigate the effect of mean stator loading on acoustic response, a series of experiments were performed in the Purdue Annular Cascade Research Facility. The run conditions were 800-rpm rotor shaft rotation, 175-ft/s ($M = 0.15$) axial velocity, and stator angles of attack ranging from -20 to 25 deg in 5 deg increments. Therefore, the rotor excitation was held constant in all cases.

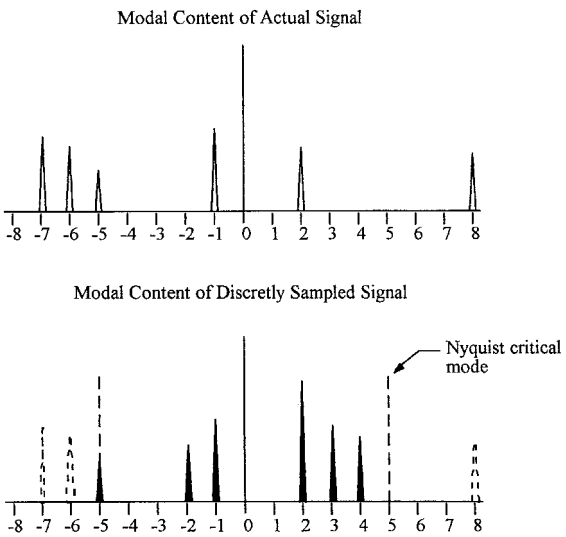

Fig. 3 Aliasing of an undersampled signal.

The modes generated by the 16-bladed rotor and the 18-vaned stator are predicted by Eq. (3), and the propagation, decay, or resonance of these modes is predicted by Eq. (4). At blade passage frequency, the spatial modes of order $k_\theta = \ldots, -20, -2, 16, 34, \ldots$ are predicted to be generated, with only the $k_\theta = -2$ mode propagating. At twice blade passage frequency, spatial modes of order $k_\theta = \ldots, -22, -4, 14, 32, \ldots$ are predicted to be generated with only the $k_\theta = -4$ mode propagating. The $k_\theta = -2$ mode generated at blade passage frequency cuts on at 734 rpm and has a phase speed of -8Ω. The $k_\theta = -4$ mode generated at twice blade passage frequency cuts on at 733 rpm and has a phase speed of -8Ω. The higher-order modes at blade passage and twice blade passage frequency are all expected to decay in the axial direction.

Stator Mean Aerodynamic Loading

To quantify the mean stage loading, the stator loading is summarized in Figs. 4, 5, and 6 in terms of the surface pressure coefficient and differential surface pressure coefficient as a function of the stator mean angle of attack. Note that even at mean angles of attack of -20 and 25 deg, the flow over the stators is not separated.

Acoustic Data

The microphone signals acquired over one rotor revolution are ensemble averaged over 200 rotor revolutions to reduce noise not linked to the rotor. Figure 7 shows the time history and the temporal Fourier transform of the ensemble-averaged data. The Fourier transform has negligible high-frequency con-

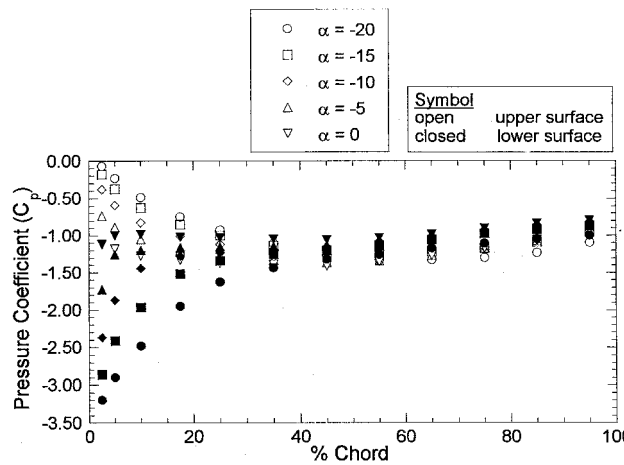

Fig. 4 Stator steady surface pressure coefficient for negative angles of attack.

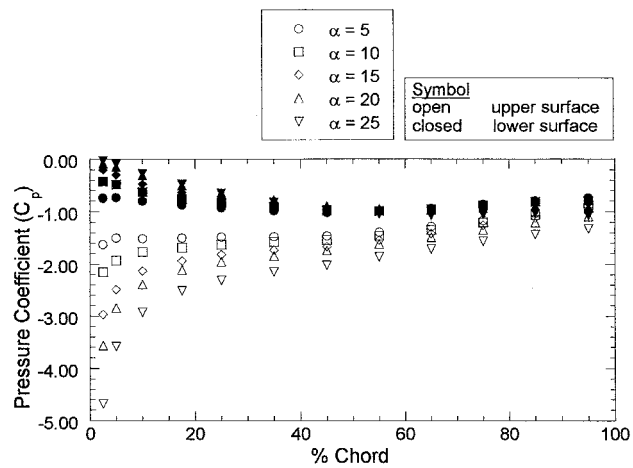

Fig. 5 Stator steady surface pressure coefficient for positive angles of attack.

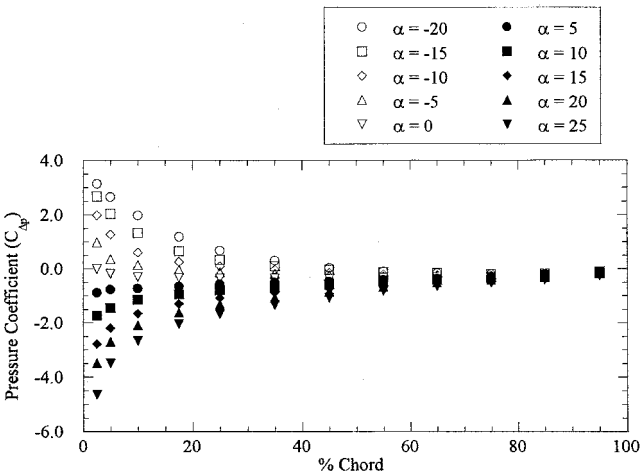

Fig. 6 Stator steady differential pressure coefficient.

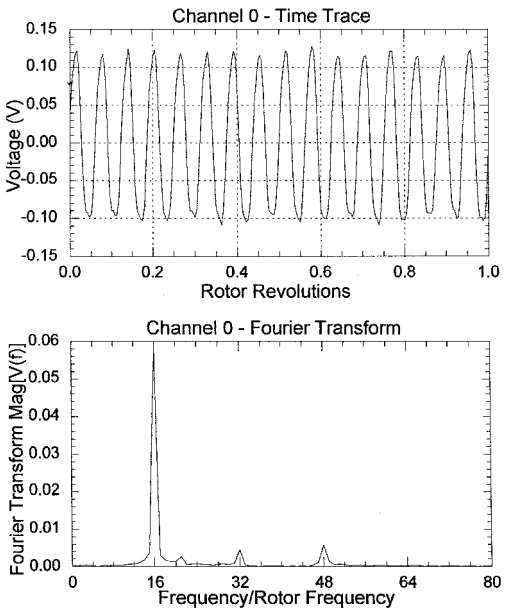

Fig. 7 Time trace and Fourier transform of ensemble-averaged signal.

tent. Primarily, the microphone signals exist at multiples of blade passage frequency, 16, 32, and 48, with the signal strength much higher at blade passage frequency than at twice blade passage frequency.

Dual discrete Fourier transforms are used to determine the acoustic pressure as a function of frequency. Data are taken for stator mean angles of attack ranging from −20 to +25 deg. The amplitude of the spatial modes at blade pass and twice blade pass frequency are then given as a function of angle of attack (Figs. 8 and 9). Recall, the $k_\theta = -2$ and -4 spatial modes are generated at blade pass and twice blade pass frequency, respectively. All other modes are either cut off and/or not generated by the rotor–stator interaction. Therefore, measurable response is only expected for $k_\theta = -2$ at blade pass and $k_\theta = -4$ at twice blade pass.

The propagating mode is expected to be of much higher amplitude than other modes that are either decaying or not generated. This expectation is realized in Fig. 8, which shows the amplitude of the spatial modes as a function of stator angle of attack. As the stator mean angle of attack is increased, the acoustic response increases quite dramatically, and as predicted, the amplitudes of all other spatial modes ($k_\theta = -5$ to -3 and -1 to 4) are negligible.

Similar results are shown in Fig. 9 for twice blade pass frequency. Again, the propagating mode that is generated by the rotor–stator interaction is considerably larger than the other modes ($k_\theta = -5$ and -3 to 4), which are either cut off or not generated by the rotor–stator interaction. Overall, the amplitude of the signals at twice blade passage frequency are only a fraction of the signals at blade passage frequency. However, the same overall trends are apparent. The propagating mode generated by the rotor–stator interaction ($k_\theta = -4$) is

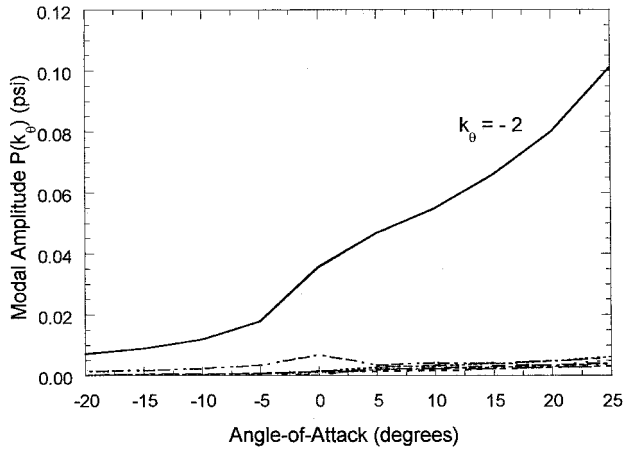

Fig. 8 Amplitude of modes generated at blade pass frequency as a function of angle of attack.

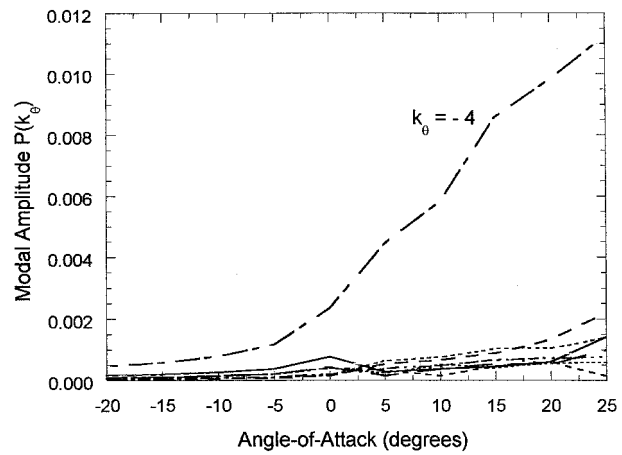

Fig. 9 Amplitude of modes generated at twice blade pass frequency as a function of angle of attack.

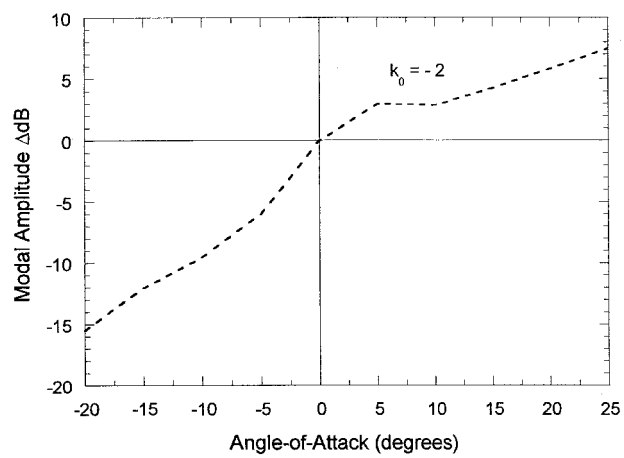

Fig. 10 Amplitude in decibels of the propagating mode at blade pass frequency relative to the zero angle-of-attack mode amplitude.

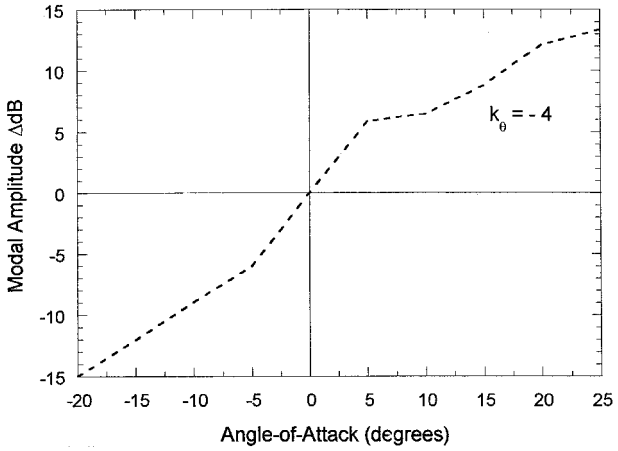

Fig. 11 Amplitude in decibels of the propagating mode at twice blade pass frequency relative to the zero angle-of-attack mode amplitude.

much larger than the other modes, and there is a dramatic increase in the acoustic response as the stator mean angle of attack is increased.

Figures 10 and 11 show the change in decibels of the propagating modes relative to zero angle of attack at blade pass frequency and twice blade pass frequency. At blade pass frequency, the amplitude of the $k_\theta = -2$ mode rises from -15 to 7 dB from -20 to 25 deg angle of attack, giving an increase of over a 20 dB. At twice blade pass frequency, the same trends are seen, where the amplitude of the $k_\theta = -4$ mode rises from -15 to 13 dB from -20 to 25 deg angle of attack, giving an increase of nearly 30 dB.

Summary and Conclusions

The objective of this experiment was to determine the influence of steady stator loading on the acoustic response of an annular cascade. This was accomplished using an circumferential array of 10 microphones installed in the inlet annulus of the Purdue Annular Cascade Research Facility. A dual spatial-temporal transform was successfully used to separate the magnitude of the spatial modes at multiples of blade passage frequency.

The analysis was performed for ensemble-averaged data, and the existence of the propagating modes was identified as having amplitudes significantly higher than modes that were not generated and/or were predicted to be cut off. Mean loading had a very significant influence in the acoustic response of the cascade. Increasing the stator mean angle of attack dramatically increased the acoustic response at blade pass and twice blade pass frequency.

Acknowledgments

This research was sponsored by NASA Lewis Research Center. Both the financial support and the technical interchanges with Dan Hoyniak are most gratefully acknowledged.

References

[1]Gliebe, P. R., "Aeroacoustics in Turbomachines and Propellers — Future Research Needs," *6th International Symposium on Unsteady Aerodynamics, Aeroacoustics, and Aeroelasticity of Turbomachines and Propellers*, edited by H. F. Atassi, Springer–Verlag, Heidelberg, Germany, 1992.

[2]Groeneweg, J. F., and Rice, E. J., "Aircraft Turbofan Noise," *Journal of Turbomachinery*, Vol. 109, No. 1, 1987, pp. 130–141.

[3]Levy, S., and Canard-Caruana, S., "Experimental Study of Noise Sources and Acoustic Propagation in a Turbofan Model," AIAA Paper 90-3950, Oct. 1990.

[4]Joppa, P. D., "Acoustic Mode Measurements in the Inlet of a Turbofan Engine," *Journal of Aircraft*, Vol. 24, No. 9, 1987, pp. 587–593.

[5]Weir, D., and Marsan, M., "Estimation of Full Scale Turbofan Engine Noise from Scale Model Fan Rig Measurements," AIAA Paper 93-4419, Oct. 1993.

[6]Heidelberg, L. J., and Hall, D. G., "Acoustic Mode Measurements in the Inlet of a Model Turbofan Using a Continuously Rotating Rake," AIAA Paper 93-0598, Jan. 1993.

[7]Hall, D. G., Heidelberg, L. J., and Konno, K., "Acoustic Mode Measurements in the Inlet of a Model Turbofan Using a Continuously Rotating Rake: Data Collection/Analysis Techniques," AIAA Paper 93-0599, Jan. 1993.

[8]Tyler, J. M., and Sofrin, T. G., "Axial Flow Compressor Noise Studies," *SAE Transactions*, Vol. 70, 1962, pp. 309–332.